



LJMU Research Online

Abadelah, M, Thevarajah, U, Ahmed, M, Seton, L, Supuk, E, Conway, BR and Larhrib, H

Novel spherical lactose produced by solid state crystallisation as a carrier for aerosolised salbutamol sulphate, beclomethasone dipropionate and fluticasone propionate

<http://researchonline.ljmu.ac.uk/id/eprint/16480/>

Article

Citation (please note it is advisable to refer to the publisher's version if you intend to cite from this work)

Abadelah, M, Thevarajah, U, Ahmed, M, Seton, L, Supuk, E, Conway, BR and Larhrib, H (2021) Novel spherical lactose produced by solid state crystallisation as a carrier for aerosolised salbutamol sulphate, beclomethasone dipropionate and fluticasone propionate. Journal of Drug

LJMU has developed **LJMU Research Online** for users to access the research output of the University more effectively. Copyright © and Moral Rights for the papers on this site are retained by the individual authors and/or other copyright owners. Users may download and/or print one copy of any article(s) in LJMU Research Online to facilitate their private study or for non-commercial research. You may not engage in further distribution of the material or use it for any profit-making activities or any commercial gain.

The version presented here may differ from the published version or from the version of the record. Please see the repository URL above for details on accessing the published version and note that access may require a subscription.

For more information please contact researchonline@ljmu.ac.uk

<http://researchonline.ljmu.ac.uk/>

1 **Novel Spherical Lactose Produced by Solid State Crystallisation as a Carrier for Aerosolised**
2 **Salbutamol Sulphate, Beclomethasone Dipropionate and Fluticasone Propionate**

3

4 Mohamad Abadelah ^{a&e}, Ursula Thevarajah ^a, Mahmud Ahmed^b, Linda Seton ^c, Enes Supuk ^d,

5 Barbara R. Conway ^a, Hassan Larhrib ^{a*}

6 ^a Department of Pharmacy, University of Huddersfield, Huddersfield, HD1 3DH, United
7 Kingdom

8 ^bHigher Institute of Science and Technology,- Tripoli, Libya

9 ^c Department of Pharmacy and Biomolecular Sciences, Liverpool John Moores University,
10 Liverpool, L3 5UX, United Kingdom

11 ^d Department of Chemical Sciences, University of Huddersfield, Huddersfield, HD1 3DH,
12 United Kingdom

13 ^e Department of Pharmacy, University of Tobruk, Libya

14

15

16

17

18

19 *Corresponding author: Department of Pharmacy, University of Huddersfield, Queensgate,
20 Huddersfield HD1 3DH, United Kingdom.

21

22 Email addresses: Ursula Thevarajah, (Thevarajah.ursula@gmail.com). Mohamad Abadelah,

23 Mohamad.Abadelah@yahoo.com , Mahmud Ahmed, Mahmud1970@hotmail.com Barbara

24 Conway B.R.Conway@hud.ac.uk, Linda Seton, L.Seton@ljmu.ac.uk, Enes Supuk, E.

25 Supuk@hud.ac.uk, Hassan Larhrib, e.larhrib@hud.ac.uk

26 **Target journal** = Journal of Drug Delivery Science and Technology (JDDST)

27

28 Number of Figures: 4 Figures

29 Number of tables: 6 Tables

30 Word count: 6109

31 -----

32 Abbreviations: SEM, Scanning electron microscopy; ESDL, Engineered Spray Dried Lactose;
33 SSC, Solid State Crystallisation; DPIs, dry powder inhalers; TED, total emitted dose; FPD, fine
34 particle dose; HPLC, high performance liquid chromatography; PIF, peak inspiratory flow;
35 Vin, inhaled volume; MMAD, mass median aerodynamic diameter; TRD, total recovered
36 dose; TRA, total residual amount.

37

38 **Abstract**

39

40 The purpose of the present work was to engineer lactose carrier particles for inhalation using a solid-
41 state crystallisation of amorphous spray dried lactose approach. A suspension of spray dried lactose was
42 contacted with hot ethanol for 10 and 30 seconds to produce spherical particles (ESDL₁₀) and (ESDL₃₀)
43 with different degrees of crystallinity, particle size, and controlled surface rugosity. Lactohale[®]
44 (control) and engineered spray dried lactose (ESDL) particles were characterised by Scanning Electron
45 Microscopy, X-ray Powder Diffraction and Tribo-electrification. Lactohale[®] and engineered lactose
46 particles were mixed separately with salbutamol sulphate (SS), beclomethasone dipropionate (BDP)
47 and fluticasone propionate (FP) and each formulation was assessed for drug content uniformity, drug
48 segregation after tribo-electrification and drug deposition using Andersen Cascade Impactor (ACI).
49 Lactohale[®] showed the highest but opposite affinity for electrical surface charges compared to
50 engineered lactose. Lactohale[®] showed the greatest variation in drug content uniformity with SS but to
51 a lesser extent with BDP and FP, whereas the ESDL carriers produced an acceptable uniform mix with
52 all drugs. SS-Lactohale[®] formulation showed the highest segregation after tribo-electrification up to
53 119-fold in comparison to that observed with SS-engineered lactose. ESDL₁₀ carrier promoted a better
54 drug deposition for both BDP and FP and showed the least variation in both content uniformity and
55 FPD with all three drugs. Therefore, production of crystalline spherical lactose carrier with controlled
56 surface texture, size and crystallinity is achievable using solid state crystallisation for DPIs, whilst
57 providing less variation in drug content uniformity and consistent fine particle dose to the lungs in-vitro
58 for both hydrophilic and hydrophobic drugs.

59 **Key words:** *Solid state crystallisation, Tribo-electrification, Salbutamol Sulphate, Beclomethasone*
60 *Dipropionate, Fluticasone Propionate*

61

62

63 1. Introduction

64 Lactose, 4-(13-D-galactosido-)-D-glucose, is commonly used excipient in oral solid dosage forms. The
65 reasons for its popularity are safety, cost-effectiveness, availability and compatibility with most drugs
66 and excipients (Steckel et al., 2004; Pilcer et al., 2010). In a solid state, lactose can either be in
67 crystalline or amorphous state. The most well-known crystalline forms are α -lactose monohydrate and
68 β -lactose. The anhydrous form also exists as α -lactose and β -lactose (Koo, 2016). A mixed crystalline
69 form of α and β lactose was also reported under specific crystallisation conditions (Larhrib et al., 2003a).
70 When crystallisation is performed at low temperatures below 93.5 °C from a supersaturated lactose
71 solution, a so-called α -lactose monohydrate is exclusively formed, whereas β -lactose is obtained at
72 temperatures over 93.5 °C (Nickerson, 1974). During crystallisation of β -lactose, no water is
73 incorporated in the crystal lattice. Therefore, the crystals of β -lactose exist in a non-hygroscopic,
74 anhydrous form only in contrast with α -lactose, which can occur both as the monohydrate and as
75 anhydrous α -lactose. Lactose is known to crystallise in an elongated shape such as tomahawk or needle
76 shape (Larhrib et al., 2003a). The tomahawk shape is obtained when the crystallisation of a
77 supersaturated α -lactose monohydrate solution is carried out slowly at ambient temperature. Elongated,
78 needle-shaped lactose crystals were also observed at high supersaturation, forcing the crystals to form
79 rapidly by precipitation, for example in the presence of a non-solvent such as acetone (Larhrib et
80 al.,2003a).

81 The aerosolisation efficiency of a powder for inhalation is highly dependent on the carrier
82 characteristics, such as particle size distribution (Kinnunen et al., 2014), particle shape (Zeng et al.,
83 2000a; Larhrib et al., 2003b) and surface properties (De Boer et al., 2012). The main objective in the
84 inhalation field is to achieve a reproducible, high pulmonary deposition. This can be achieved by
85 successful carrier selection and careful process optimisation (Pilcer et al., 2012). It is known that the
86 attractive forces between drug and carrier particles can be shape dependent (Mullins et al.,
87 1992; Crowder et al., 2001). In vitro inhalation studies have indicated that elongated (Larhrib et al.,
88 2003b; Zeng et al., 2000a), needle-like (Ikegami et al., 2002), porous and wrinkled particles (Chew et
89 al., 2005) have improved lung deposition properties of various formulations. Larhrib et al., (2003b)

90 found that as the elongation ratio of lactose carrier was increased, the flow of the carrier was reduced
91 and consequently impacted on content uniformity of salbutamol sulphate and as the result the drug
92 emission from the inhaler device was also affected. A spherical shaped lactose carrier can be more
93 preferred compared to other carrier shapes, because its good flowability and contact area between the
94 spherical particles and adhered particles is less than non-spherical particles (Cooley, et al., 2018). It
95 was reported that spherical pollen-shaped hydroxyapatite carrier increased dispersibility of budesonide
96 particles due to a reduction in particle interactions (Hassan et al., 2010).

97 Spherical particles are desirable to produce solid dosage forms due to their good flow properties and
98 consistent drug loading capacity in comparison to other shapes. Unfortunately, spherical shaped lactose
99 is challenging to produce by crystallisation from solution in comparison to other shapes. Some
100 techniques, such as spray drying, are known to produce hollow and spherical particles but a drawback
101 is the formation of amorphous content. Therefore, the first aim of the present work was to produce novel
102 hollow engineered spherical crystalline lactose carrier particles with controlled size, surface properties
103 and crystallinity using solid state crystallisation (SSC). The Engineered Spray Dried Lactose (ESDL)
104 and Lactohale[®] (control) were then characterised using Scanning Electron Microscopy (SEM), X-ray
105 Powder Diffraction (XRD) and Triboelectrification. The second aim was to investigate the suitability
106 of this novel lactose as a carrier for DPIs with hydrophilic and hydrophobic model drugs, namely,
107 salbutamol sulphate (SS), beclomethasone dipropionate (BDP) and fluticasone propionate (FP)

108 **2. Materials and Methods**

109 **2.1 Materials**

110 Micronized salbutamol sulphate (VMD= 2.4 μm), beclomethasone dipropionate (VMD= 2.3
111 μm) and fluticasone propionate (VMD= 4.3 μm) (GSK, UK) were used as model drugs.
112 Lactose α -monohydrate (Lactohale[®] 200) was purchased from DFE Pharma, UK. Ethanol,
113 Absolute was purchased from Fisher Scientific, UK. Ultrapure water system was purchased
114 from Thermo Fisher scientific, UK.

115 **2.2 Methods**

116 - *Preparation of Lactohale® Carrier*

117 Lactohale® was sieved to obtain a relatively narrow size distribution (63-90µm) to match
118 approximately the particle size of Engineered Spray Dried Lactose (ESDL). Lactose is brittle,
119 and as a result, the powder was sieved manually and slowly for about 30 minutes to limit the
120 particle abrasion, breakage and tribo-charging effect which can occur during a conventional
121 mechanical sieving. The powder was then collected in a sealed glass jar and stored in a
122 desiccator over silica gel until required for further investigation.

123 - *Production of Spray-Dried Lactose Particles*

124 A pre-determined amount of Lactohale® was dissolved in ultra-pure water at room temperature
125 to obtain 10% w/v lactose solution. The resulting lactose solution was spray-dried using a
126 laboratory scale spray dryer (SD-06 spray-dryer, Labplant, UK). The spray drying conditions
127 were inlet temperature 180°C; outlet temperature of 102°C; solution feed rate 4rpm (2ml/min);
128 air pressure: (3 bars); 0.5mm spray nozzle. The spray-dried lactose was recovered from the
129 collecting jar and transferred into a glass vial before storing in a desiccator over silica-gel until
130 required.

131 - *Solid State Crystallisation of Spray Dried Lactose.*

132 A 100 ml of absolute ethanol (Fisher, UK) was poured into a 600mL glass beaker and
133 transferred to the fume hood, where ethanol was allowed to boil using a hot plate (Cole-
134 Parmer®, UK). A pre-determined quantity of spray-dried lactose particles (about 10 g) was
135 introduced into the hot solvent for 10 seconds while stirring the lactose suspension at 250 rpm.
136 The beaker was then removed from the hot plate and the lactose suspension was filtered using
137 a 500µm sieve into a collecting pan to remove any aggregates. The recovered crystallised
138 spray-dried lactose suspension was dispersed using cool air generated by a hair drier to avoid
139 polymorphic transformation which can be caused by the application of heat. This step was

140 followed by drying the ESDL in a ventilated oven at 45°C for 48 hours (Mettler, Germany).
141 The particles were collected from the collecting pan as a free-flowing powder and allowed to
142 cool to room temperature for 1 hour before being transferred to a clean sealed glass jar and
143 stored in a desiccator over silica gel until required. The particles resulting from this batch were
144 named Engineered Spray Dried Lactose (ESDL₁₀).

145 The same process was repeated for a second spray dried lactose batch however, the spray-dried
146 particles were left in contact with hot ethanol for a longer period of time of 30 seconds. The
147 particles resulting from this batch were named Engineered Spray Dried Lactose (ESDL₃₀).

148 - *Preparation of Powder Blends:*

149 Each drug, SS, FP and BDP (Glaxo Smith Kline, Ware, UK) 40 ± 1.45 mg was mixed
150 separately with 2.7 g Lactohale[®] and ESDL in a ratio of 1:67.5 w/w, in accordance with the
151 ratio employed in the commercial Ventolin[®] formulation so that each capsule contained 400
152 ± 14.5 μ g of drug and 27 mg lactose. Thus, each drug was weighed into a 20ml glass vial to
153 which was added approximately an equivalent amount of lactose carrier, either Lactohale[®] or
154 ESDL and blended manually using a microspatula. Then more lactose carrier was added similar
155 to the amount of the blend contained in the glass vial and mixed manually using the same
156 microspatula. This process was repeated until all the lactose carrier (2.70 g) was added into the
157 drug/lactose blend to obtain a ratio of drug to carrier of 1:67.5 w/w. The same process was
158 applied to all formulations irrespective of the drug or carrier. The stoppered vials were then
159 placed in a Turbula mixer (Turbula[®], UK) and mixed at 72 min⁻¹ for 5 min, 10 min, 15 min and
160 30 min. Finally, the samples were stored at room temperature in a vacuum desiccator over silica
161 gel until required for further investigation. Hard gelatine capsules (size 3) were filled with
162 exactly 27.4 ± 0.5 mg of the powder mixture so that each capsule contained 400 ± 14.5 μ g of
163 the drug. The filling of the capsules was completed manually.

164 - *Measurement of the Homogeneity of the Mixtures*

165 The drug content uniformity of SS, FP and BDP and lactose mixes were determined by taking
166 randomly 10 aliquots of approximately 27.4 mg each (3 from the top, 3 from the middle, 3
167 from the bottom and one randomly from the blend). Each aliquot was poured into a 100 mL
168 volumetric flask and made up to volume with acetonitrile: water (75:25 v/v) for FP and BDP
169 and 30:70 % v/v methanol and 10 mM hexane sulfonic acid adjusted to pH 2.5 with glacial
170 acetic acid for SS. Each solution was assayed for drug content using validated HPLC methods
171 (Thevarajah, 2019). The average mean recovery as % of the nominal dose was calculated and
172 the percentage coefficient of variation (% CV) was the metric used to assess the content
173 uniformity of each powder blend.

174 - *Characterisation of Particle Shape and Size using Scanning Electron*
175 *Microscopy (SEM)*

176 SEM was used to assess morphological features: particle size, shape, and surface appearance,
177 for Lactohale[®] and ESDL. The particles were then coated with approximately 15 to 20 nm gold
178 for one minute using an ion sputter coater (Quorum Technologies Ltd., UK) under vacuum of
179 0.09 mbar and a current of 40mA. Micrograph images were produced by scanning fields,
180 selected randomly at several magnifications with a Jeol 6060LV SM scanning electron
181 microscope (JEOL, Japan).

182 - *Solid State Characterisation of Lactohale[®] and ESDL using X-Ray Powder*
183 *Diffraction (XRPD)*

184 X-Ray powder diffraction was used to assess the crystallinity of lactose particles. Powder X-
185 ray diffraction patterns were recorded after samples were spread uniformly over the sample
186 holder using a D8 Advance powder X-Ray diffractometer with Cu K α radiation of $\lambda = 1.54\text{\AA}$
187 (Bruker AXS). The voltage and current applied were 40 kV and 40 mA, respectively. The
188 sample powder was packed into the rotation sample holder and scanned in the 2θ range 5° to

189 60°. Crystallinity was identified by comparing the characteristic 2 θ peaks (“fingerprints”) of
190 the XRD pattern.

191 - *Measurement of Triboelectric Charges*

192 The charge-to-mass ratio (Q/M) of the DPI formulations was assessed using a tribo-electric
193 device based on a shaking concept consisting of a Faraday cup, an electrometer, and a shaking
194 machine (Retsch MM400), previously described (Šupuk et. al., 2009). The Faraday cup
195 consists of two concentric cups made of a conducting material. The concentric cups differ in
196 size: the outer cup is larger and acts as a shield to prevent impact of external electric fields.
197 The inner cup was connected to an electrometer (Keithley, model 6514, UK) as per the method
198 described by Secker and Chubb, (1984). The powders used for this study already possessed a
199 certain level of residual charge, referred to as the initial charge, which was measured first,
200 without shaking, by placing a 0.1g of each powder into the Faraday cup connected to an
201 electrometer. This charge was the result of powder being in contact with surfaces before the
202 experiments were conducted. In this work, the initial charge was relatively small compared to
203 the final charge. The final charge was obtained by weighing DPI powder (0.1 g for each run,
204 n=3) and loading the powder inside a cylindrical stainless steel container (10 ml) before being
205 shaken in a horizontal direction using the shaking machine. The powder sample was then
206 poured into the Faraday cup and the net charge (C) present on the powder particles was
207 measured on the electrometer. The charge values were presented in nano-coulombs per gram
208 (nC/g) as the mean charge-to-mass ratio (Q/M). This was calculated by dividing the final
209 charge with the final mass of the respective powder. The maximum charge-to-mass level was
210 attained to ensure the effect of the initial charge was negligible. The shaking was carried out at
211 a vibration frequency of 20 Hertz in order to induce tribo-electrification inside the container.
212 The maximum charge-to-mass ratio acquired for Lactohale[®] and ESDL and their respective

213 formulation blends was 2 minutes after shaking. Measurements were repeated three times to
214 ensure reliable data was produced.

215 The same procedure was followed for all DPI formulations. The Retsch shaking cylindrical
216 container was cleaned thoroughly after each measurement with isopropyl alcohol to ensure the
217 removal of any residual particles, surface charge from a previous test and impurities which
218 could invalidate the results. Isopropyl alcohol was allowed to evaporate before further tests
219 were carried out. The experiment was carried out in a controlled environment with an ambient
220 temperature of 20-23 °C and relative humidity (RH) of 32-39 %.

221 - *Aerodynamic Dose Emission Characteristics of SS, BDP And FP*
222 *Formulations using Andersen Cascade Impactor (ACI)*

223 The formulations blend of SS, BDP and FP with Lactohale, ESDL₁₀ and ESDL₃₀ aerodynamic
224 dose emission characteristics was assessed *in-vitro* using compendial dose emission testing for
225 DPIs. A vacuum pump was used to generate an inhalation flow with a constant peak inspiratory
226 flow (PIF) that corresponds to a 4 kPa pressure drop across the inhaler device with an inhaled
227 volume of 4 L (USP, 2014). Breezhaler[®] is a low resistance device and a PIF exceeding 100
228 L/min is required to achieve a pressure drop inside device equivalent to 4kPa when using the
229 device (Abadelah, 2017). The ACI (Copley Scientific, UK) was calibrated at three PIFs 28.3 ,
230 60 and 90 L/min, therefore, in the present study the inspiratory parameters used were PIF of
231 90 L/min and inhaled volume (V_{in}) of 4 L to be in accordance with the calibrated range of
232 ACI. The ACI was connected to a vacuum pump (HCP5, Copley Scientific Ltd, UK) via the
233 critical flow controller (model TPK; Copley Scientific Ltd, UK). The ACI stages were
234 assembled with 10 mL of 75 % acetonitrile: 25 % ultra-purified water (% v/v) in the pre-
235 separator and a glass fibre GF50 (Whatman; UK) filter was placed in the final stage. For each
236 determination, one dose was prepared and aerosolised according to the manufacturer's
237 recommendations in patient information leaflet (PIL). Three separate determinations were

238 made for each formulation blend at a set PIF and Vin. Once the dose aerosolised into the ACI,
239 a washing procedure took place to recover the API (SS, BDP and FP) from the mouthpiece,
240 induction port, pre-separator, ACI stages, filter, capsule, and device. A validated HPLC method
241 was used to quantify the amount of the API (SS, BDP and FP) deposited in each part in the
242 ACI as well as the residual amount left in the device and capsule.

243 - *Drug Quantification using HPLC Method*

244 The Shimadzu HPLC system comprised a liquid chromatograph (LC-20AT), an auto sampler
245 (SIL-20A), a column oven (CTO-10ASVP), a UV-VIS detector (SPD-20A).

246 The HPLC method for the detection of SS was a mobile phase of 30:70 % v/v methanol and
247 10 mM hexane sulfonic acid adjusted to pH 2.5 with glacial acetic acid, SS was detected using
248 a detection wavelength of $\lambda = 276\text{nm}$. The mobile phase for BDP and FP was 75:25 % v/v
249 Acetonitrile: water using a detection wavelength of $\lambda = 230\text{ nm}$. For both methods, the
250 stationary phase was Luna[®] column C18 100A (250mm x 4.6 mm) with a pore size of 5 μm
251 (Phenomenex, UK), the flow rate was 1mL/min, and the injection volume of the sample was
252 20 μl . The retention time for SS, FP and BDP was 10.5, 2.8 and 6.5 mins, respectively. The
253 LOD for SS, BDP and FP were 0.66 $\mu\text{g/mL}$, 0.62 $\mu\text{g/mL}$ and 0.23 $\mu\text{g/mL}$, while the LOQ was
254 2 $\mu\text{g/mL}$, 1.89 $\mu\text{g/mL}$, and 0.75 $\mu\text{g/mL}$

255 - *Data Analysis*

256 The Copley Inhaler Testing Data Analysis Software (CITDAS version 2.0, Copley Scientific
257 Ltd, UK)) was used to calculate the aerodynamic dose emission parameters. The total emitted
258 dose (TED) was obtained from the cumulative amounts of API (SS, BDP and FP) deposited in
259 the mouthpiece (MP), induction port (IP), using the USP throat, the pre-separator (PS) and all
260 the stages of the ACI. The fine particle dose (FPD) was the mass associated with particles < 5
261 μm . Large particle mass (LPM) was sum of the drug amount deposited in the upper part of the

262 ACI (MP + IP + PS). Total residual amount (TRA) was the sum of the dose left in the device
263 and capsule after the inhalation manoeuvre. The total recovered dose (TRD) was the sum of
264 the total emitted dose (TED) and the total residual amount (TRA). A one way and two way
265 ANOVA, as well as Tuckey test, were carried out. The statistical analysis comprised of a one
266 way and two-way factorial analysis of variance (ANOVA) which was carried out using the
267 statistical analysis software, SPSS Statistics (SPSS Inc., Chicago, USA) and Excel Microsoft®
268 data analysis.

269 **3. Results and Discussion**

270 *3.1 Characterization of Carrier Particle Size, Shape and Surface Texture*

271

272 Solid state crystallisation (SSC) of the spray dried Lactohale® lactose particles resulted in the
273 formation of spherical particles with a modified surface texture as opposed to spray dried
274 Lactohale® lactose and tomahawk Lactohale® particles with a smoother surface (Figures. 1).
275 The ESDL particles can be produced with different surface rugosity without altering the shape
276 of the particles. The time of exposure of spray-dried particles to hot ethanol was found to be a
277 critical factor in altering surface rugosity as shown in SE micrographs (Figure 1 C and D). The
278 spray dried particles were engineered using two exposure times to hot ethanol, 10 seconds, and
279 30 seconds, to produce ESDL₁₀ and ESDL₃₀, respectively. The longer the exposure time to
280 ethanol the rougher, larger, and more porous the particles. Therefore, ESDL₃₀ was larger,
281 rougher, and more porous than ESDL₁₀. The performance of DPIs is greatly influenced by the
282 physical properties of the carrier, particularly their particle size, morphology/shape, and surface
283 roughness. As these factors are interdependent, it is difficult to completely understand how
284 they individually influence DPI performance (Peng et al., 2016). SSC is predictable in
285 maintaining the original shape of the spray dried particles. Furthermore, the surface roughness

286 can be adjusted using different exposure times to hot ethanol to produce particles with desired
287 surface rugosity so as to provide enough adhesion of drug to the carrier, which is necessary in
288 the production of a stable, homogeneous powder blend with acceptable drug content
289 uniformity, yet allowing easy drug detachment from the surface of the carrier during inhalation
290 manoeuvre.

291 Increasing the temperature in the crystallisation medium is expected to enhance the solubility
292 of lactose, especially very fine lactose particles and amorphous regions within lactose, thus
293 reducing the supersaturation of lactose in the crystallisation medium. Initially, an excess of
294 spray dried particles (10 g) were introduced into the crystallisation medium with a solvent in
295 which the solubility of lactose is not substantially affected, in order to maintain the
296 supersaturation of lactose in the crystallisation medium. Undissolved lactose would act as a
297 seed for crystal growth. It is important to note that increasing temperature reduces the viscosity
298 of the crystallisation medium, thus facilitating the transfer of the dissolved lactose solution
299 onto the lactose seeds for crystal growth. Increasing the time from 10 seconds to 30 seconds
300 affected surface texture of the particles forming rough, porous, spherical particles. The initial
301 spherical shape of lactose is maintained but the particles have increased in size as shown from
302 scanning electron micrographs of spray dried lactose (Figure 1b) in comparison to ESDL₁₀
303 (Figure 1d) and ESDL₃₀ (Figure 1c). Thus, ESDL₃₀ are larger than ESDL₁₀ which are
304 significantly larger than spray dried lactose. The hollow volume is significantly larger for
305 Engineered lactose suggesting that the particles expanded in radial direction and both the
306 temperature and time of exposure to the solvent acted as an inflating agent to expand the size
307 of the particles.

308 Pharmaceutical powders are generally divided into three categories depending on their
309 deformation behaviour: plastic, elastic, and brittle. Lactose is known to be brittle as suggested
310 from its high mean yield pressure derived from Heckel plot (Heckel, 1961; Roberts and Rowe,

311 1985). During crystal growth, the hollow volume of ESDL increases and reaches a maximum
312 volume after which the particles burst. The increase in the hollow volume is dictated by the
313 plasto-elasticity of the material. As the growth of the particles progresses, the porous structure
314 of the particles facilitates permeation of the solvent inside the hollow space, thus causing an
315 increase in the vapour pressure inside the particles caused by the evaporation of the solvent.
316 The vapour pressure built inside the hollow space of the particle exerts a radial stress on the
317 shell. If the radial stress exceeds a certain limit, the particle will either expand by plastic or
318 elastic deformation or burst if the shell resists deformation as is the case with a fragmenting
319 powder. Lactose is a fragmenting material and increasing the exposure time of the particles to
320 the solvents beyond 30 seconds caused them to burst to form needle shape particles as they
321 could not withstand the radial stress applied from inside the particles. The vapour pressure
322 increases in a radial direction and equally so that the spherical shape of the particles is
323 maintained. Thus, SSC allows a great control of particle size, surface properties and
324 crystallinity of particles.

325 *Assessment of Crystallinity*

326 Crystalline solids lead to the diffraction of X-rays at a unique combination of angles, enabling
327 identification of the material. Lactohale[®] is crystalline with diffraction peaks at 12°; 16° and
328 19° (Figure 2a) representative of the crystalline form of α -lactose monohydrate (Gombas et
329 al., 2002)

330 In the spray drying process, the liquid feed is atomised into very small droplets through a
331 narrow nozzle within a hot drying gas. The rapid evaporation of the droplets results in solid
332 amorphous particles. Spray drying is highly scalable and offers high precision control of
333 particle size and bulk density, but the major drawback is the formation of amorphous material
334 which is unstable and can revert back to crystalline material with aging or when exposed to
335 humidity (Wu, et al., 2014).

336 Spray dried lactose exhibits a broad “halo” effect with no noticeable diffraction, allowing it to
337 be clearly distinguished from crystalline Lactohale (Figure 2b). Spray-drying is known to
338 produce predominantly amorphous material because the transition between the liquid and solid
339 phase is instantaneous (Santos et al., 2018) in other words, the rapid drying of the lactose solute
340 droplet did not allow sufficient time for lactose to form a crystalline structure. Amorphous
341 material tends to be highly cohesive (Young et al., 2007), have a poor flow and is
342 thermodynamically unstable (Shen et al., 2010). The hollow spray dried particles have a
343 significant advantage over solid non-hollow particles, the low density of hollow drug particles
344 have attracted interest in the inhalation field. They provide significant improvements in lung
345 targeting and dose consistency, relative to current marketed inhalers (Weers and Tarara, 2014).
346 The spray dried lactose particles produced in this work are hollow, but too small to be used as
347 a carrier in DPI formulations. Engineered spray dried lactose particles in the presence of hot
348 ethanol increased their particle size, volume (Figure 1) and restored the crystallinity to the
349 particles (Figure 2). The hollow nature of lactose particles may impart low density to lactose
350 carrier particles to provide them with a long time of flight so that they can travel longer distance
351 in the airstream before impaction, thus giving opportunity for drug particles to detach from
352 their surface to maximise drug deposition. The relative degree of crystallinity of different
353 samples of the same crystal form is usually proportional to the ratio of the peak intensity (Zeng
354 et al., 2000). It is interesting to note that higher peak intensities were observed on ESDL₃₀
355 diffractogram (Figure 2c) suggesting that ESDL₃₀ was more crystalline than ESDL₁₀ (Figure
356 2d). It is clear that prolonging the exposure time to ethanol has an impact on the crystallinity
357 of the ESDL particles, since it has been reported that an increase in temperature has a linear
358 relationship with the degree of crystallinity of lactose particles (Chiou et al., 2007).

359 **3.2. Drug-Carrier Formulation Assessment:**

360 *3.2.1 Drug Content Uniformity*

361 Content uniformity is a critical determinant that helps ensure the strength of the drug in the
362 formulation remains within the specified acceptance limits and to assess the quality of a batch
363 (Williams, Adams, Poochikian, & Hauck, 2002).

364 Blending uniformity of the binary mixtures varied significantly ($p < 0.05$) with mixing
365 times, drug types and the type of carrier (Tables 1, 2 and 3). The mean (SD) drug weight
366 uniformity varied between 359.54 (15.83) μg and 416.92 (8.36) μg for all batches, which are
367 within the acceptable limit of 90-110% of the target weight [FDA, 1988]. However, mixing
368 time can have a significant effect on the % CV. Of the three drugs investigated, SS was found
369 to have the greatest deviation in the % CV with increasing the mixing time from 5 mins to 30
370 mins mainly with Lactohale[®] (Table 1) with a corresponding % CV of 1.04 and 9.69 at 5mins
371 and 30 mins respectively. A short mixing time of 5 minutes provided a better repartition of SS
372 particles on the surface of Lactohale[®] as shown from the low % CV of 1.04 %. The
373 morphological features of particles are known to affect the blend uniformity (Venables &
374 Wells, 2001). Carrier particles with high elongation ratio are disadvantageous in DPI dose
375 metering and processing at handling scale due to their poor flowability (Larhrib et al., 2003a;
376 Kaialy et al., 2011). Spherical agglomerates were shown to facilitate drug loading, improve
377 the flowability of the powder and improved the blend uniformity (Zellnitz et al., 2021).

378 Furthermore, smooth carrier particles have a low loading capacity which can promote drug
379 segregation especially for high dose drugs. Lactohale[®] has an elongated shape with a smooth
380 surface (Figure 1a), these morphological features may have affected both the adhesion of drug
381 to the carrier and the flow of powder inside the Turbula mixer, facilitating segregation between
382 drug and carrier particles by prolonging the mixing time.

383 Both BDP and FP achieved a smaller %CV with prolonged mixing time with Lactohale[®] in
384 comparison to SS (Table 1). BDP and FP are both hydrophobic and their extent of adhesion to
385 the carrier may be different to hydrophilic drugs such as SS. It is clear that drug content

386 uniformity does not depend only on the nature of the carrier but also on the drug adherence to
387 the carrier. SS mixes and de-mixes rapidly when mixed with Lactohale[®]. Hydrophobic drugs
388 such as BDP and FP are highly cohesive and require longer time of mixing and high shear
389 forces to break up drug aggregates before distributing uniformly on the lactose carrier. Thus,
390 hydrophobic drugs can benefit from prolonged mixing times to provide good content
391 uniformity than hydrophilic drugs such as SS with Lactohale[®]. Generally, ESDL particles were
392 spherical in shape with a rough surface and gave the highest homogeneity with a low %CV
393 compared with tomahawk shaped smooth Lactohale[®], whether with SS, FP or BDP (Table 2
394 and 3).

395 *3.2.2 Tribo-Charging Behaviours of Carriers Lactohale[®], ESDL₁₀ And ESDL₃₀; Drugs*
396 *SS, FP, BDP and their Respective Formulations*

397 The carriers, drugs and their blend with carriers were assessed for their triboelectrification
398 using a Faraday cup coupled to an electrometer and the results are summarised in Table 4. The
399 results from the Tribo-charging showed that API materials charge to a higher extent with much
400 greater variability than is seen with excipients which agrees with previous studies using the
401 same technique (Supuk et. al., 2012). Table 4 indicates that different carriers have different
402 charging behaviours. The results show that Lactohale[®] was negatively charged with a specific
403 charge of -15.38 ± 17.89 (nC/g), whereas ESDL₃₀ and ESDL₁₀ were positively charged with a
404 specific charge of 5.39 ± 1.23 and 1.06 ± 2.43 (nC/g), respectively.

405 Murtomaa et al. (2002) noticed that the specific charge of lactose decreases as a function of the
406 amorphous content. This is in agreement with the finding of the present work, and there is
407 direct correlation between the specific charge of lactose carrier and XRD data (Figure 2).
408 Lactohale[®] was most crystalline and exhibited the highest specific charge, whereas ESDL₁₀
409 was the least crystalline and exhibited the lowest specific charge (Table 4). This shows that the
410 charge distribution on carrier surface is also influenced by its crystallinity. ESDL₁₀ and ESDL₃₀

411 are spherical whereas Lactohale[®] is an elongated tomahawk shape, therefore, electrical charges
412 may distribute homogeneously on the surface of spherical particles, whereas most charges may
413 concentrate on the tips and edges of tomahawk elongated carrier particles. Since charging
414 behaviour is a surface phenomenon, this will eventually influence the interactions between
415 drugs and carrier particles and could inherently influence adhesion and agglomeration of
416 particles as well as *in-vitro* drug deposition (Bennett et al., 1999).

417 Lactohale[®] alone or in the formulation with SS, FP or BDP always exhibited negative charge.
418 The electronegative charge on Lactohale[®] increased even more when formulated with SS
419 particles, the charge increased from -15.38 ± 17.89 nC/g for Lactohale[®] alone to -25.68 ± 2.60
420 nC/g when formulated with SS. Mixing SS to Lactohale[®] carrier particles charged the
421 formulation more negatively, this could be due to segregation of the binary blend, which was
422 supported by drug content uniformity data (Tables 1) showing an increase in the % CV with
423 increasing mixing time. The particle motion inside the shaking container represents a unique
424 system in that it describes triboelectrification in every aspect, i.e., friction through sliding,
425 impact on the walls and between particles, and collisions by particles rolling. In order to assess
426 the largest contributor to charge generation by tribo-electrification in a given application, the
427 method of charging should yield the total saturated charge. A shaking container considers the
428 whole of powder sample to avoid bias sampling and a rate process is involved to confirm that
429 saturation level has been reached. The use of electrometer and a Faraday cup set up means that
430 a high sensitivity of charge measurements is obtained. Following tribo-electric charging tests
431 to determine the saturation level, it was found that particles adhered to the inner surface of the
432 shaking container. The adhesion of powders to the contact surface may cause changes in the
433 composition of the powders during tribo-electric charging and ultimately affect the
434 homogeneity of the sample. The particles which adhere to the container surfaces may also
435 cause variations in the interactions of free moving particles and therefore prolong powders

436 reaching their saturated value early in the tribo-electrification process. The saturated charge-
437 to-mass values and adhesion data obtained using the shaking concept may provide important
438 information when new inhaler devices and formulations are designed in order to improve the
439 drug deposition. The exact effect of such particle charge and adhesion on inhalation
440 performance needs to be further investigated.

441

442 3.3.3 *Assessment of Deaggregation of Drug Particles by Measuring Drug Amounts* 443 *Recovered from the Wall of the Shaker*

444 Table 5 showed that the amount of drug recovered from the walls of the shaking container after
445 tribo-electrification for all DPI formulations was found to be dependent on the nature of the
446 carrier and the drug used. For example, SS-Lactohale[®] formulation showed the highest amount
447 of drug adhesion to the stainless steel container with an average value of $1051.3 \pm 13.86 \mu\text{g}$
448 corresponding to approximately 72% of SS recovered from the wall of the shaker. However,
449 the amount of SS was significantly reduced to $135.21 \pm 1.27 \mu\text{g}$ for SS-ESDL₃₀ and $28.56 \pm$
450 $0.43 \mu\text{g}$ for SS-ESDL₁₀ corresponding to 88 and 119 fold reduction in SS for SS-ESDL₃₀ and
451 SS-ESDL₁₀, respectively (Table 5). SS-Lactohale[®] formulation showed the highest drug
452 recovered from the stainless steel container and also showed the highest variation in drug
453 content uniformity with increasing mixing time (Table 1). SS-ESDL₃₀ and SS-ESDL₁₀ showed
454 less drug adhesion to the wall of shaking container (Table 5) but also less % CV in drug content
455 uniformity in comparison to SS-Lactohale[®] (Tables 2 and 3). Therefore, the tribo-electric
456 charging device based on the shaking concept may provide a rapid mean for screening DPI
457 formulations less prone to segregation that provide a stable mix for good drug content
458 uniformity. Drug adhesion to the tribo-electrification stainless steel shaker was dependent not
459 only on the carrier but also on the drug. BDP and FP are both hydrophobic drugs and when
460 mixed with Lactohale[®] showed a substantial reduction in the amount of drug adhered to the

461 cell shaker (Table 5). The degree of adhesion to Lactohale[®] carrier is stronger compared to SS
462 providing a stable mix and as confirmed by the drug content uniformity study (Table 1) where
463 both BDP and FP showed generally smaller % CV when compared to SS-Lactohale[®]. The
464 tribo-electrification drug de-aggregation assessment study (Table 5) corroborates with drug
465 content uniformity study (Tables 1,2 and 3) demonstrating that drug adhesion to the wall of the
466 shaker could be mainly caused by segregation of drug weakly adhering to the carrier.

467

468 3.3.4 *In-Vitro* Aerodynamic Dose Emission Characteristics Study of SS, BDP And FP with 469 Lactohale[®] and Engineered Carriers (ESDL₁₀ And ESDL₃₀).

470 It is widely accepted that breath activated DPIs are often associated with flow rate dependent
471 changes in the emitted dose and also the aerodynamic characteristics such as the fine particle
472 dose (FPD) and mass median aerodynamic diameter (MMAD) (Abadelah et al., 2017;
473 Abadelah et al., 2018).

474 In the present study, we investigated the deposition profiles of SS, BDP and FP after
475 formulating each drug separately with Lactohale[®] and engineered carriers ESDL₁₀ and ESDL₃₀.
476 The three model drugs (SS, BDP, FP) showed different charging behaviour in tribo-
477 electrification study (Figure 3) and different degrees of adhesion to the wall of the stainless
478 steel shaker (Table 5). The carriers: Lactohale[®], ESDL₁₀ and ESDL₃₀ showed differences in
479 their morphological features (crystallinity, surface charges, surface roughness and shape) all of
480 which may influence drug adhesion and detachment during aerosolisation. The carrier is a
481 major component in DPI formulations, and it is critical to design a carrier with desired
482 morphological features to provide sufficient adhesion with drug particles to form a stable mix
483 with acceptable drug content uniformity, yet to allow drug detachment from its surface during
484 the inhalation manoeuvre.

485 SS behaved differently in its deposition profile with the three carriers, providing the highest
486 FPD (156.78 ± 2.62) with Lactohale[®] in comparison to ESDL₁₀ FPD (79.48 ± 1.40) and ESDL₃₀
487 FPD (100.21 ± 1.61) (Figure 4). SS–Lactohale[®] formulation showed the greatest variation in
488 drug content uniformity (Table 1) and the highest amount of drug adhering to the wall of the
489 stainless steel shaker in the Tribo-electrification study (Table 5). The high FPD for SS–
490 Lactohale[®] formulation (Figure 4) are in line with the triboelectrification study (Table 5),
491 suggesting weak adhesion of SS to Lactohale[®] promoting drug detachment during inhalation
492 manoeuvre. The weak adhesion between SS and Lactohale[®] is also reflected in the amount of
493 SS adhered to capsule and device (total residual amount, TRA) which was significantly higher
494 ($p < 0.05$) ($52.31 \pm 4.26 \mu\text{g}$) for Lactohale[®] in comparison to ($44.52 \pm 3.18 \mu\text{g}$) and ($35.00 \pm$
495 $2.57 \mu\text{g}$) for ESDL₁₀ and ESDL₃₀, respectively.

496 The rank order of FPD for BDP and FP was ESDL₁₀ > Lactohale[®] > ESDL₃₀ (Table 6). Despite
497 Lactohale[®] performing better with SS formulation in terms of FPD, its performance was worse
498 than ESDL₁₀ with BDP and FP, this shows that there is no universal carrier that performs very
499 well and equally with all drugs, i.e., a carrier may perform well with one drug but not
500 necessarily perform well with other drugs. However, for all three drugs tested, ESDL₁₀ showed
501 the least variation in the FPD when compared with Lactohale[®] and ESDL₃₀.

502 BDP and FP results showed that nearly 50% of the nominal dose $400\mu\text{g}$ deposited as large
503 particle mass (LPM) in the upper part of the impactor (Table 6), this is in accordance with
504 previous studies (Mohammed et al., 2012, Abadelah et al., 2017). MMAD values ranged
505 between 1.6 and $2.6 \mu\text{m}$ (Table 6). An MMAD $< 5 \mu\text{m}$ is considered to be necessary for
506 sufficient airway deposition (Mitchell et al., 1987).

507 Geometric standard deviation (GSD) values were $> 1.2 \mu\text{m}$ (Tables 6) suggesting
508 polydispersity of the aerosol, this common for drug particles generated by micronisation, which
509 is the case for all the model drugs used in this work. Drug retention inside the inhaler continues

510 to be a factor plaguing the performance of novel inhalers (Tajber et al., 2009). Drug retention
511 varies between inhaler devices in that some studies have reported between 30-50% of the
512 nominal dose being retained within the device (Heng et al., 2013). It is important that the
513 complete dose is released from the inhaler to maximise the therapeutic effect, minimising drug
514 wastage and avoiding potential dosage errors during the next inhalation. The lowest TRA for
515 both BDP and FP was observed with ESDL₁₀, suggesting lower amount of drug retained in the
516 capsule and device.

517 **4. Conclusion**

518 A novel hollow, crystalline, spherical lactose carrier was produced using a solid-state
519 crystallisation technique from a spray-dried lactose suspension in hot ethanol. This novel
520 crystallisation technique is more predictable in forming spherical shaped particles with desired
521 size, crystallinity, surface charge, hollow and surface rugosity. Engineered spray dried Lactose
522 (ESDL) particles were formed with different sizes, hollow volume, crystallinity, and surface
523 rugosity. The longer the time where particles are exposed to hot ethanol, the larger the size,
524 hollow, crystallinity, and surface rugosity. The plasto-elasticity of the outer shell of the
525 particles can dictate the final inner hollow volume of a particle and hence particle size.
526 Engineered lactose ESDL₁₀ and ESDL₃₀ showed less variation in drug content uniformity
527 compared to Lactohale[®] when formulated with SS, BDP and FP. The results from the tribo-
528 electric charging device show all formulations formed with ESDL₁₀ and APIs produce the most
529 stable blends with lowest charge-to-mass ratio. The triboelectrification device may provide a
530 rapid means for screening DPI formulations less prone to segregation that provide a stable mix
531 for good drug content uniformity. Lactohale[®] was the most suitable carrier for SS in providing
532 high FPD, but care must be taken in optimising the mixing procedure to ensure an acceptable
533 drug content uniformity. ESDL₁₀ carrier promoted a better drug deposition for both BDP and
534 FP and showed the least variation in both content uniformity and FPD irrespective of the model

535 drug when compared to Lactohale and ESDL₃₀. Therefore, production of crystalline spherical
536 lactose carrier is achievable using solid state crystallisation. The surface texture, size and
537 crystallinity can be easily controlled to achieve the optimal spherical carrier for DPIs providing
538 less variation in drug content uniformity and consistent fine particle dose to the lungs in-vitro
539 for both hydrophilic and hydrophobic drugs.

540 **Conflict of interest**

541 All authors declare no conflicts of interest in this work.

542

543

544

545

546

547

548

549

550

551

552

553

554

555

556

557

558

559

560

561

562 **References**

563

564

565

566

567

568

569

570

571

572

573 Abadelah, M., Chrystyn, H., Bagherisadeghi, G., Abdalla, G., & Larhrib, H. (2018). Study of
574 the emitted dose after two separate inhalations at different inhalation flow rates and
575 volumes and an assessment of aerodynamic characteristics of indacaterol Onbrez
576 Breezhaler® 150 and 300 µg. *AAPS PharmSciTech*, 19(1), 251-261.. AAPS
577 PharmSciTech. <https://doi.org/10.1208/s12249-017-0841-y>

578 Abadelah, M., Hazim, F., Chrystyn, H., Bagherisadeghi, G., Rahmoune, H., & Larhrib, H.
579 (2017). Effect of maximum inhalation flow and inhaled volume on formoterol drug
580 deposition in-vitro from an Easyhaler® dry powder inhaler. *European Journal of*
581 *Pharmaceutical Sciences*, 104, 180-187. <https://doi.org/10.1016/j.ejps.2017.03.035>

582 Bennett, F. S., Carter, P. A., Rowley, G., & Dandiker, Y. (1999). Modification of
583 electrostatic charge on inhaled carrier lactose particles by addition of fine
584 particles. *Drug Development and Industrial Pharmacy*.
585 <https://doi.org/10.1081/DDC-100102148>

586 Chew, N. Y. K., Shekunov, B. Y., Tong, H. H. Y., Chow, A. H. L., Savage, C., Wu, J.,
587 & Chan, H. K. (2005). Effect of amino acids on the dispersion of disodium
588 cromoglycate powders. *Journal of Pharmaceutical Sciences*.
589 <https://doi.org/10.1002/jps.20426>

590 Cooley, M., Sarode, A., Hoore, M., Fedosov, D. A., Mitragotri, S., & Gupta, A. S. (2018).
591 Influence of particle size and shape on their margination and wall-adhesion:
592 implications in drug delivery vehicle design across nano-to-micro
593 scale. *Nanoscale*, 10(32), 15350-15364. <http://doi.org/10.1039/c8nr04042g>

594 Crowder, T. M., Louey, M. D., Sethuraman, V. V., SMYTH, H. C., & Hickey, A. J. (2001).
595 2001: An odyssey in inhaler formulation and design. *Pharmaceutical*
596 *technology*, 25(7), 99-113.

597 Dal Negro, R. W. 2015. Dry powder inhalers and the right things to remember: a concept
598 review. *Multidisciplinary respiratory medicine*, 10, 1. 1-4
599 <https://doi.org/10.1186/s40248-015-0012-5>

- 600 De Boer, A. H., Chan, H. K., & Price, R. (2012). A critical view on lactose-based drug
601 formulation and device studies for dry powder inhalation: which are relevant and
602 what interactions to expect?. *Advanced drug delivery reviews*, 64(3), 257-274.
603 [http://doi.org/ 10.1016/j.addr.2011.04.004](http://doi.org/10.1016/j.addr.2011.04.004).
- 604 FDA. 1998. Food and Drug Administration; Guidance for Industry Metered Dose Inhaler
605 (MDI) and Dry Powder Inhaler (DPI) Drug Products [Online]. Available:
606 https://www.fda.gov/ohrms/dockets/ac/00/backgrd/3634b1c_sectiond.pdf [Accessed 5
607 June 2020].
- 608 Hassan, M. S., & Lau, R. (2010). Inhalation performance of pollen-shape carrier in dry
609 powder formulation with different drug mixing ratios: Comparison with lactose
610 carrier. *International journal of pharmaceutics*, 386(1-2), 6-14.
611 <http://doi.org/10.1016/j.ijpharm.2009.10.047>
- 612 Heckel, R. W. (1961). Density-pressure relationships in powder compaction. *Trans*
613 *Metall Soc AIME*, 221(4), 671-675.
- 614 Heng, D., Lee, S. H., Ng, W. K., Chan, H.-K., Kwek, J. W. and Tan, R. B. 2013. Novel
615 alternatives to reduce powder retention in the dry powder inhaler during
616 aerosolization. *International journal of pharmaceutics*, 452, 194-200. [http://doi.org/](http://doi.org/10.1016/j.ijpharm.2013.05.006)
617 [10.1016/j.ijpharm.2013.05.006](http://doi.org/10.1016/j.ijpharm.2013.05.006)
- 618 Ikegami, K., Kawashima, Y., Takeuchi, H., Yamamoto, H., Isshiki, N., Momose, D. I., &
619 Ouchi, K. (2002). Improved inhalation behavior of steroid KSR-592 in vitro with
620 Jethaler® by polymorphic transformation to needle-like crystals (â-form).
621 *Pharmaceutical Research*. <https://doi.org/10.1023/A:1020492213172>
- 622 Kaialy, W., Alhalaweh, A., Velaga, S. P., & Nokhodchi, A. (2011). Effect of carrier
623 particle shape on dry powder inhaler performance. *International Journal of*
624 *Pharmaceutics*. <https://doi.org/10.1016/j.ijpharm.2011.09.010>
- 625 Kinnunen, H., Hebbink, G., Peters, H., Shur, J., & Price, R. (2014). An investigation into the
626 effect of fine lactose particles on the fluidization behaviour and aerosolization
627 performance of carrier-based dry powder inhaler formulations. *AAPS*
628 *PharmSciTech*, 15(4), 898-909. [http://doi.org/ 10.1208/s12249-014-0119-6](http://doi.org/10.1208/s12249-014-0119-6)
- 629 Koo, O. M. (Ed.). (2016). *Pharmaceutical excipients: properties, functionality, and*
630 *applications in research and industry*. John Wiley & Son
- 631 Larhrib, H., Martin, G. P., Marriott, C., & Prime, D. (2003b). The influence of carrier and
632 drug morphology on drug delivery from dry powder formulations. *International*
633 *Journal of Pharmaceutics*. [https://doi.org/10.1016/S0378-5173\(03\)00156-X](https://doi.org/10.1016/S0378-5173(03)00156-X)
- 634 Larhrib, H., Martin, G. P., Prime, D., & Marriott, C. (2003a). Characterisation and deposition
635 studies of engineered lactose crystals with potential for use as a carrier for aerosolised
636 salbutamol sulfate from dry powder inhalers. *European Journal of Pharmaceutical*
637 *Sciences*. [https://doi.org/10.1016/S0928-0987\(03\)00105-2](https://doi.org/10.1016/S0928-0987(03)00105-2)
- 638 Mitchell, D., Solomon, M., Tolfree, S., Short, M. and Spiro, S. 1987. Effect of particle size
639 of bronchodilator aerosols on lung distribution and pulmonary function in patients
640 with chronic asthma. *Thorax*, 42, 457-461. [http://doi.org/ 10.1136/thx.42.6.457](http://doi.org/10.1136/thx.42.6.457)

- 641 Mohammed, H., Roberts, D. L., Copley, M., Hammond, M., Nichols, S. C. and Mitchell, J.
642 P. 2012. Effect of sampling volume on dry powder inhaler (DPI)-emitted aerosol
643 aerodynamic particle size distributions (APSDs) measured by the Next-Generation
644 Pharmaceutical Impactor (NGI) and the Andersen Eight-Stage Cascade Impactor
645 (ACI). *AAPS PharmSciTech*, 13, 875-882.
- 646 Mullins, M. E., Michaels, L. P., Menon, V., Locke, B., & Ranade, M. B. (1992). Effect of
647 geometry on particle adhesion. *Aerosol Science and Technology*.
648 <https://doi.org/10.1080/02786829208959564>^[1]_{SEP}
- 649 Murtomaa, M., Ojanen, K., Laine, E., & Poutanen, J. (2002). Effect of detergent on
650 powder triboelectrification. *European Journal of Pharmaceutical Sciences*.
651 [https://doi.org/10.1016/S0928-0987\(02\)00167-7](https://doi.org/10.1016/S0928-0987(02)00167-7)
- 652 Nickerson, T. A., & Moore, E. E. (1974). Factors influencing lactose crystallization. *Journal*
653 *of Dairy Science*, 57(11), 1315-1319. [https://doi.org/10.3168/jds.S0022-](https://doi.org/10.3168/jds.S0022-0302(74)85061-7)
654 [0302\(74\)85061-7](https://doi.org/10.3168/jds.S0022-0302(74)85061-7).
- 655 Peng, T., Lin, S., Niu, B., Wang, X., Huang, Y., Zhang, X., ... & Wu, C. (2016).
656 Influence of physical properties of carrier on the performance of dry powder
657 inhalers. *Acta pharmaceutica sinica B*, 6(4), 308-318.
658 <https://doi.org/10.1016/j.apsb.2016.03.011>
- 659 Pilcer, G., & Amighi, K. (2010). Formulation strategy and use of excipients in pulmonary
660 drug delivery. *International Journal of Pharmaceutics*.
661 <https://doi.org/10.1016/j.ijpharm.2010.03.017>^[1]_{SEP}
- 662 Roberts, R. J., & Rowe, R. C. (1985). The effect of punch velocity on the compaction
663 of a variety of materials. *Journal of pharmacy and pharmacology*, 37(6), 377-
664 384. <https://doi.org/10.1111/j.2042-7158.1985.tb03019>
- 665 Santos, D., Maurício, A. C., Sencadas, V., Santos, J. D., Fernandes, M. H., & Gomes, P. S.
666 (2018). Spray drying: An overview. Pignatello, R.(Comp.). *Biomaterials-Physics and*
667 *Chemistry-New Edition*. InTech. UK, 9-35.<http://doi.org/10.5772/intechopen.72247>
- 668 Secker, P. E., & Chubb, J. N. (1984). Instrumentation for electrostatic
669 measurements. *Journal of electrostatics*, 16(1), 1-19.
670 [https://doi.org/10.1016/0304-3886\(84\)90015-9](https://doi.org/10.1016/0304-3886(84)90015-9)
- 671 Shen, S. C., Ng, W. K., Chia, L., Dong, Y. C., & Tan, R. B. H. (2010). Stabilized amorphous
672 state of ibuprofen by co-spray drying with mesoporous SBA-15 to enhance dissolution
673 properties. *Journal of Pharmaceutical Sciences*. <https://doi.org/10.1002/jps.21967>
- 674 Steckel, H., & Bolzen, N. (2004). Alternative sugars as potential carriers for dry powder
675 inhalations. *International Journal of Pharmaceutics*.
676 <https://doi.org/10.1016/j.ijpharm.2003.10.039>^[1]_{SEP}
- 677 Supuk, E., Seiler, C., & Ghadiri, M. (2009). Analysis of a simple test device for tribo-electric
678 charging of bulk powders. *Particle and Particle Systems Characterization*.
679 <https://doi.org/10.1002/ppsc.200800015>
- 680 Supuk, E., Zarrebini, Z., Reddy, J. P., Hughes, H., Leane, M., Tobyn, M.J., Timmins, P., &
681 Ghadiri, M. (2012). Tribo-electrification of active pharmaceutical ingredients and
682 excipients. *Powder Technology*. <https://doi.org/10.1016/j.powtec.2011.10.059>

683 Tajber, L., Corrigan, O. and Healy, A. 2009. Spray drying of budesonide, formoterol
684 fumarate and their composites—II. Statistical factorial design and in vitro deposition
685 properties. *International Journal of Pharmaceutics*, 367, 86-96. [http://doi.org/
686 10.1016/j.ijpharm.2008.09.029](http://doi.org/10.1016/j.ijpharm.2008.09.029)

687 Thevarajah, U. (2019). Engineered inflated spherical lactose particle and its potential use as a
688 carrier for dry powder formulation aerosols (Doctoral dissertation, University of
689 Huddersfield). <http://eprints.hud.ac.uk/id/eprint/34918>
690 USP 2014. United States Pharmacopeia, USP 38-NF 33.

691 Venables, H. J., & Wells, J. I. (2001). Powder mixing. *Drug development and industrial
692 pharmacy*, 27(7), 599-612. <https://doi.org/10.1081/DDC-100107316>

693 Weers, J., & Tarara, T. (2014). The PulmoSphere™ platform for pulmonary drug
694 delivery. *Therapeutic delivery*, 5(3), 277-295. [http://doi.org/ 10.4155/tde.14.3](http://doi.org/10.4155/tde.14.3).

695 Williams, R. L., Adams, W. P., Poochikian, G., & Hauck, W. W. (2002). Content
696 uniformity and dose uniformity: Current approaches, statistical analyses, and
697 presentation of an alternative approach, with special reference to oral inhalation
698 and nasal drug products. *Pharmaceutical Research*.
699 <https://doi.org/10.1023/A:1015114821387>

700 Wu, L., Miao, X., Shan, Z., Huang, Y., Li, L., Pan, X., ... & Wu, C. (2014). Studies on the
701 spray dried lactose as carrier for dry powder inhalation. *asian journal of
702 pharmaceutical sciences*,9(6), 336-341. <https://doi.org/10.1016/j.ajps.2014.07.006>

703 Young, P. M., Chiou, H., Tee, T., Traini, D., Chan, H. K., Thielmann, F., & Burnett, D.
704 (2007). The use of organic vapor sorption to determine low levels of amorphous
705 content in processed pharmaceutical powders. *Drug development and industrial
706 pharmacy*, 33(1), 91-97. <https://doi.org/10.1080/03639040600969991>

707 Zellnitz, S., Lamešić, D., Stranzinger, S., Pinto, J. T., Planinšek, O., & Paudel, A. (2021).
708 Spherical agglomerates of lactose as potential carriers for inhalation. *European
709 Journal of Pharmaceutics and Biopharmaceutics*, 159, 11-20.
710 <https://doi.org/10.1016/j.ejpb.2020.12.015>

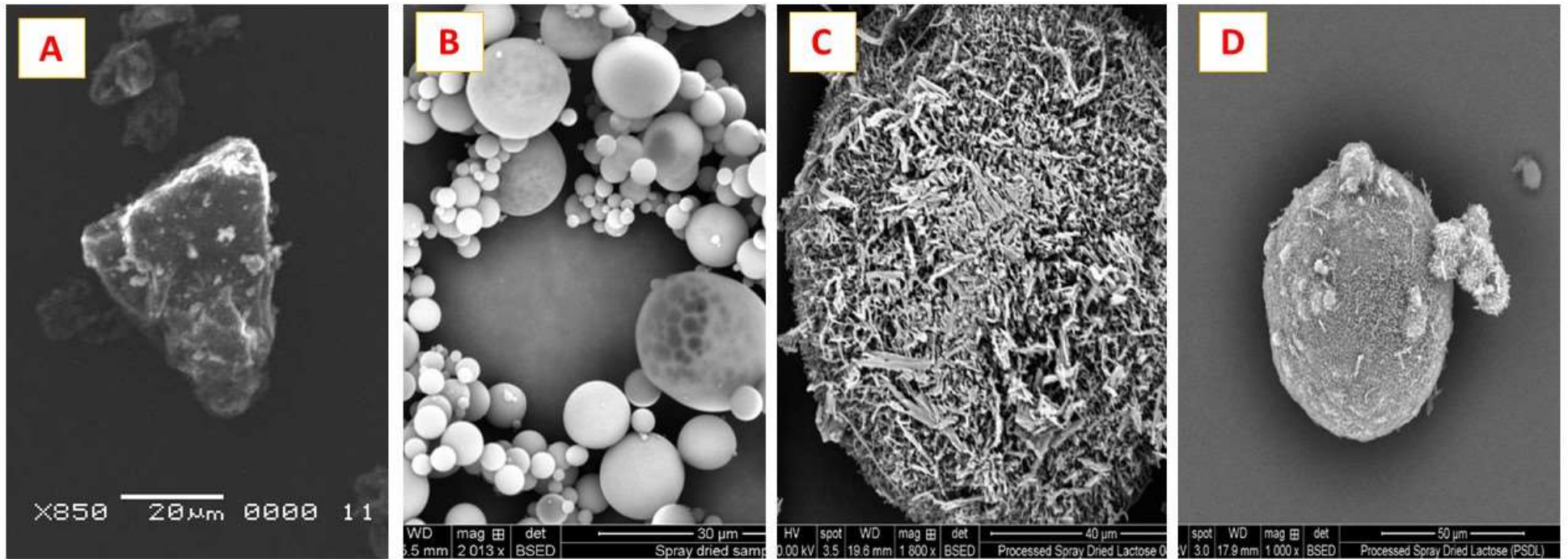
711 Zeng, X. M., Martin, G. P., Marriott, C., & Pritchard, J. (2000a). The effects of carrier size
712 and morphology on the dispersion of salbutamol sulphate after aerosolization at
713 different flow rates. *The Journal of Pharmacy and Pharmacology*.
714 <https://doi.org/10.1211/0022357001777342>

715 Zeng, X. M., Martin, G. P., Marriott, C., & Pritchard, J. (2000b). The influence of carrier
716 morphology on drug delivery by dry powder inhalers. *International Journal of
717 Pharmaceutics*. [https://doi.org/10.1016/S0378-5173\(00\)00347-1](https://doi.org/10.1016/S0378-5173(00)00347-1)^[1]_{SEP}

718
719
720
721

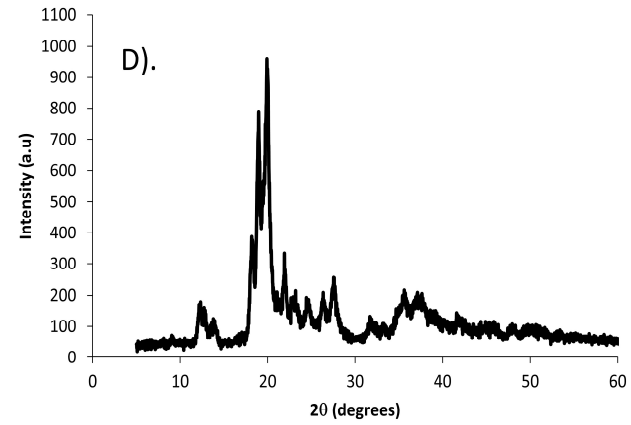
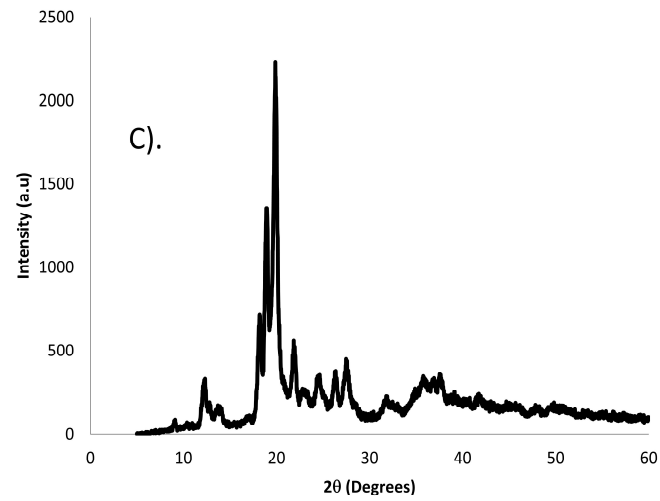
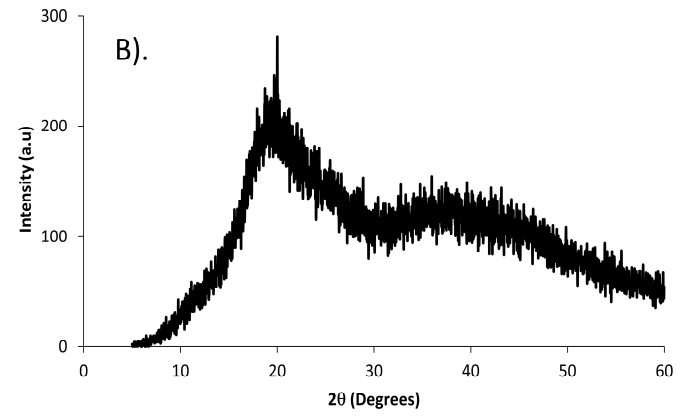
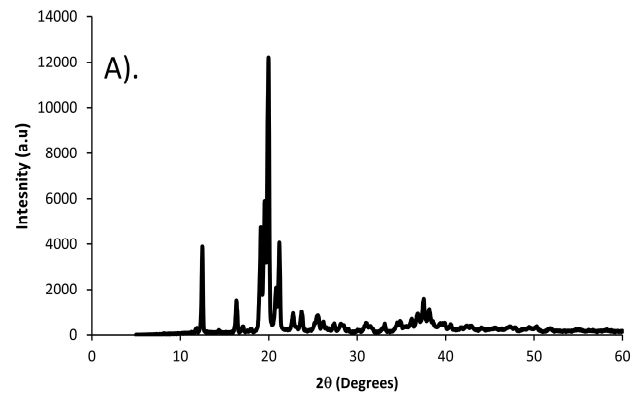
722
723
724
725

List of Figure Captions:



726
727
728
729

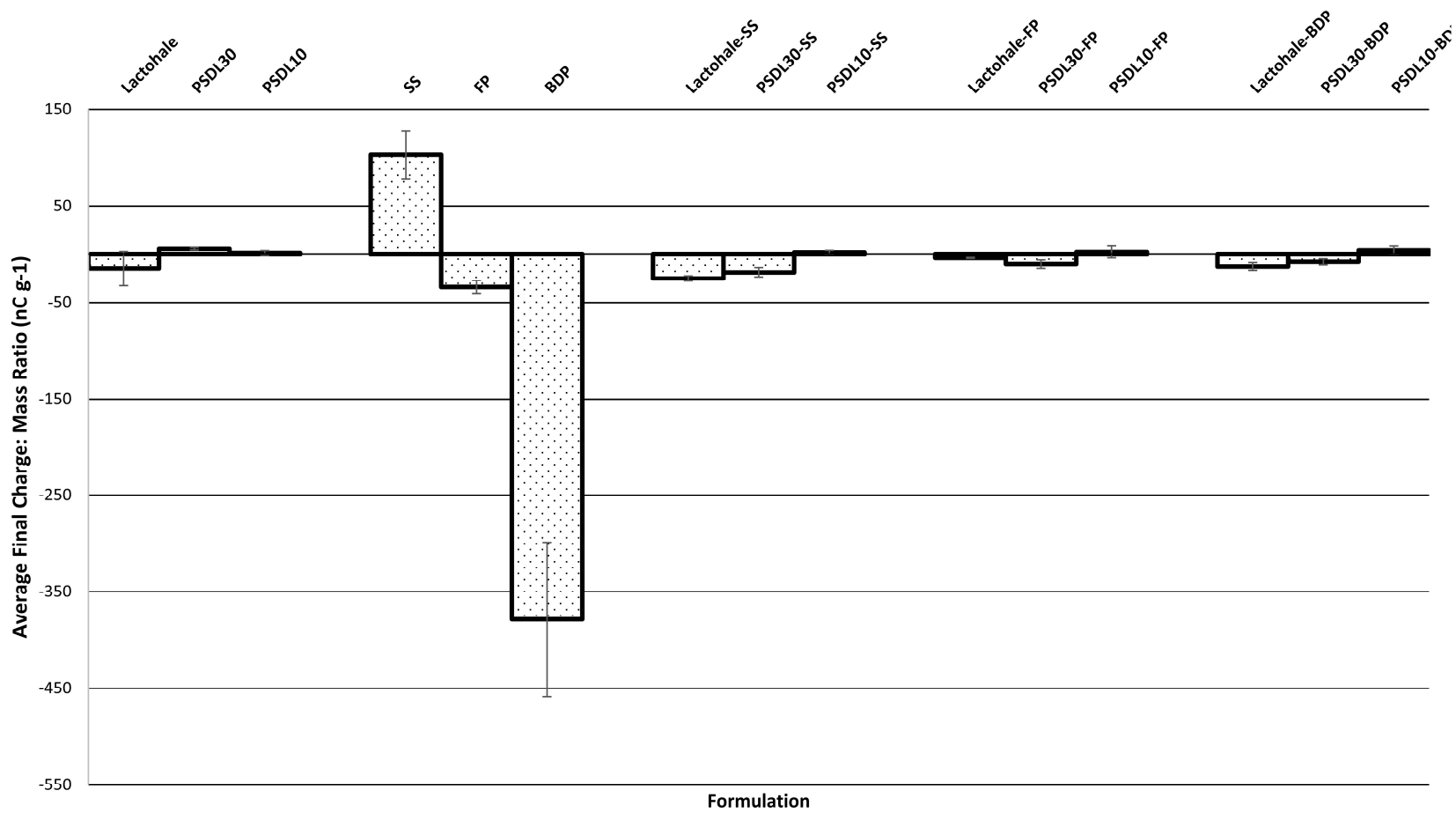
Figure 1: Scanning electron micrographs of A) Lactohale[®], B) spray dried Lactohale[®], C) Engineered spray dried lactose (ESDL₃₀), D) Engineered spray dried lactose (ESDL₁₀).



730

731

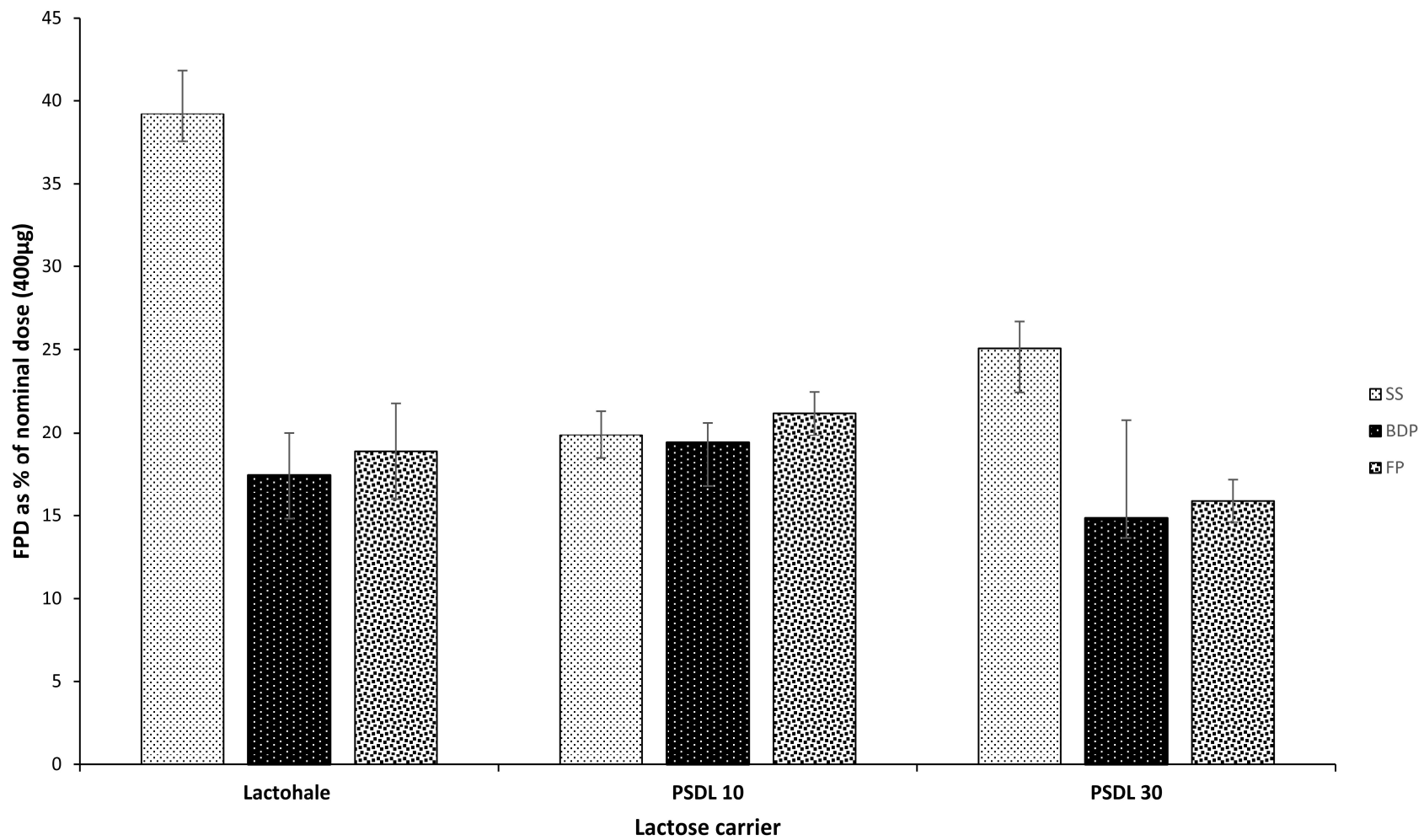
Figure 2: X-ray diffraction pattern of [A) Lactohale® (63-90 μm) particles, B) spray dried lactose, C) ESDL₃₀ and D) ESDL₁₀ [n=3].



732

733

Figure 3: The average final charge: mass ratios (nC g⁻¹) of carriers, drugs, and formulations after tribo-electrification [n=3].



734
735
736

Figure 4: Mean (SD) of Fine particle dose (FPD) of SS, BDP and FP with Lactohale®, ESDL₁₀ and ESDL₃₀ .[n=3].

737

738 **Table 1:** Content uniformity of SS, FP and BDP in µg with Lactohale® at different mixing
739 times: 5, 10, 15 and 30 mins [n=10].

Lactohale®						
Time	BDP		FP		SS	
	Amount in µg Mean (SD)	% CV	Amount in µg Mean (SD)	% CV	Amount in µg Mean (SD)	% CV
5 Min	396.78(24.73)	6.23	412.86(6.57)	1.59	404.48(4.23)	1.04
10 Min	359.54(15.83)	4.40	406.67(5.79)	1.42	409.85(25.53)	6.23
15 Min	399.00(13.65)	3.42	414.27(7.31)	1.76	408.66(37.95)	9.29
30 Min	405.85(16.55)	4.08	416.78(15.53)	3.72	410.33(1.05)	9.69

740

741 **Table 2:** Content uniformity of SS, FP and BDP in µg with ESDL₁₀ at different mixing times: 5,
742 10, 15 and 30 mins[n=10].

ESDL ₁₀						
Time	BDP		FP		SS	
	Amount in µg Mean (SD)	% CV	Amount in µg Mean (SD)	% CV	Amount in µg Mean (SD)	% CV
5 Min	404.76(11.56)	2.85	409.67(3.40)	0.83	408.81(14.56)	3.32
10 Min	405.21(8.63)	2.13	398.16(6.11)	1.53	413.64(11.91)	2.88
15 Min	416.29(15.43)	3.71	398.79(6.24)	1.56	403.42(11.12)	2.75
30 Min	406.71(14.73)	3.62	406.06(14.64)	3.60	398.81(9.68)	2.28

743

744 **Table 3:** Content uniformity of SS, FP and BDP in µg with ESDL₃₀ at different mixing times: 5,
745 10, 15 and 30 mins [n=10].

ESDL ₃₀						
Time	BDP		FP		SS	
	Amount in µg Mean (SD)	% CV	Amount in µg Mean (SD)	% CV	Amount in µg Mean (SD)	% CV
5 Min	425.10(15.36)	3.61	407.51(5.20)	1.28	414.64(14.79)	3.57
10 Min	412.37(10.32)	2.50	416.92(8.36)	2.00	404.80(9.57)	2.36
15 Min	404.45(9.87)	2.44	412.32(9.13)	2.21	408.31(20.61)	5.05
30 Min	402.93(10.45)	2.59	406.23(17.84)	4.39	392.23(19.41)	4.95

746

747

748

749

750

751

752

753
754

Table 4: The average final charge-to-mass ratios of the formulations after tribo-electrification. [n=3]

Formulation	Average final charge: mass ratio (nC g⁻¹)
Lactohale®	-15.38 ± 17.89
ESDL₃₀	5.39 ± 1.23
ESDL₁₀	1.06 ± 2.43
SS	102.79 ± 24.67
FP	-34.52 ± 6.59
BDP	-378.77 ± 80.25
SS-Lactohale®	-25.68 ± 2.60
SS-ESDL₃₀	-19.39 ± 4.88
SS-ESDL₁₀	1.75 ± 2.02
FP-Lactohale®	-4.51 ± 0.53
FP-ESDL₃₀	-10.93 ± 4.29
FP-ESDL₁₀	2.01 ± 6.40
BDP-Lactohale®	-13.35 ± 3.96
BDP-ESDL₃₀	-8.49 ± 3.14
BDP-ESDL₁₀	3.91 ± 4.27

755
756
757
758
759
760
761
762
763
764
765
766
767
768
769

770 **Table 5:** The average drug content of SS, FP and BDP recovered from the wall of the
 771 stainless-steel shaker after tribo-charging measurements (n=3)
 772

Formulation	amount (μg)	SD	% Recovery \pm SD
SS-L	1051.31	13.86	71.9 \pm 0.95
SS-ESDL₃₀	135.21	1.27	9.26 \pm 0.09
SS-ESDL₁₀	28.56	0.43	1.96 \pm 0.03
BDP-L	11.9	2.06	0.8 \pm 0.14
BDP-ESDL₃₀	1.95	0.26	0.13 \pm 0.01
BDP-ESDL₁₀	24.93	0.42	1.71 \pm 0.02
FP-L	8.83	2.94	0.6 \pm 0.2
FP-ESDL₃₀	0.81	0.06	0.05 \pm 0.0
FP-ESDL₁₀	57.08	0.1	3.9 \pm 0.0

773
 774
 775
 776
 777
 778
 779
 780
 781
 782
 783
 784
 785
 786
 787
 788
 789
 790
 791

792
793
794

Table 6: Mean (SD) of aerodynamic dose emission characteristics of SS, BDP and FP with Lactohale[®], ESDL₁₀ and ESDL₃₀ at a PIF of 90 L/min and Vin of 4 L using ACI [n=3].

	Lactohale[®]	ESDL₁₀	ESDL₃₀
SS deposition			
MP	2.51(0.36)	16.49(2.56)	5.22(0.29)
IP	41.64(2.71)	94.77(2.69)	44.29(2.90)
PS	95.29(6.44)	136.35(5.91)	165.96(3.24)
LPM	139.77(3.29)	247.61(2.89)	215.47(5.16)
FPD	156.78(2.62)	79.48(1.40)	100.21(1.61)
TED	309.22(2.97)	337.04(3.50)	328.52(3.27)
TRA	52.31(3.72)	44.52(2.21)	35.00(2.61)
TRD	361.53(3.09)	382.31(3.30)	363.51(2.67)
MMAD (µm)	1.60(0.00)	2.00(0.10)	1.90(0.00)
GSD	2.27(0.06)	2.40(0.00)	2.47(0.06)
BDP deposition			
MP	12.90(2.61)	17.74(0.52)	6.49(0.41)
IP	53.41(6.04)	96.53(2.64)	100.85(0.26)
PS	132.78(7.06)	133.26(3.92)	132.65(5.51)
LPM	199.09(4.39)	247.53(7.88)	239.90(12.06)
FPD	69.66(2.60)	77.58(1.20)	59.38(5.90)
TED	277.27(1.56)	340.72(2.70)	307.69(2.29)
TRA	51.63(5.08)	23.98(1.19)	80.32(9.61)
TRD	328.89(2.37)	364.70(2.10)	388.02(2.45)
MMAD (µm)	1.93(0.06)	2.30(0.10)	2.67(0.06)
GSD	2.27(0.25)	2.70(0.90)	1.90(0.02)
FP deposition			
MP	6.75(0.78)	17.02(0.48)	17.87(0.97)
IP	90.24(3.49)	84.49(2.28)	120.89(4.74)
PS	146.89(5.77)	125.12(3.62)	109.19(6.98)
LPM	243.87(8.41)	226.63(6.01)	247.95(7.49)
FPD	75.49(2.90)	84.61(1.30)	63.47(1.82)
TED	332.43(2.52)	323.57(2.30)	324.36(1.76)
TRA	59.78(2.37)	26.38(3.30)	58.85(2.09)
TRD	392.21(3.79)	349.95(2.30)	383.22(2.17)
MMAD (µm)	2.67(0.06)	2.30(0.12)	1.80(0.00)
GSD	2.17(0.06)	2.5(0.00)	2.93(0.06)

795
796